Dye Sensitization of Nanocrystalline Titanium Dioxide with Square Planar Platinum(II) Diimine Dithiolate Complexes

Ashraful Islam, Hideki Sugihara,* Kohjiro Hara, Lok Pratap Singh, Ryuzi Katoh, Masatoshi Yanagida, Yoshiaki Takahashi, Shigeo Murata, and Hironori Arakawa*

Photoreaction Control Research Center, National Institute of Advanced Industrial Science and Technology (AIST), AIST Tsukuba Central 5, 1-1-1 Higashi, Tsukuba, Ibaraki 305-8565, Japan

Gaku Fujihashi

Sumitomo Osaka Cement Company, Ltd., 585 Toyotomi, Hunabashi, Chiba 274-8601, Japan

Received April 12, 2001

A series of platinum-based sensitizers of the general type Pt(NN)(SS), where NN is 4,4′-dicarboxy-2,2′-bipyridine (dcbpy) or 4,7-dicarboxy-1,10-phenanthroline (dcphen) and SS is ethyl-2-cyano-3,3-dimercaptoacrylate (ecda), quinoxaline-2,3-dithiolate (qdt), 1,2-benzenedithiolate (bdt), or 3,4-toluenedithiolate (tdt), that have various ground-state oxidation potentials has been synthesized and anchored to nanocrystalline titanium dioxide electrodes for light-to-electricity conversion in regenerative photoelectrochemical cells with an I^-/I^-_3 acetonitrile electrolyte. The intense mixed-Pt/dithiolate-to-diimine charge-transfer absorption bands in this series could be tuned from 440 to 580 nm by choosing appropriate dithiolate ligands, and the highest occupied molecular orbitals varied by more than 500 mV. Spectrophotometric titration of the Pt(dcphen)(bdt) complex exhibits a ground-state pK_a value of 3.2 ± 0.1, which can be assigned to the protonation of the carboxylate group of the dcphen ligand. Binding of Pt(dcbpy)(qdt) to porous nanostructured TiO_2 films was analyzed using the Langmuir adsorption isotherm model, yielding an adsorption equilibrium constant of 4×10^5 M^{-1}. The amount of dye adsorbed at the surface of TiO_2 films was 9.5×10^{-8} mol/cm^2, which is ca. 50% lower than the full monolayer coverage. The resulting complexes efficiently sensitized TiO_2 over a notably broad spectral range and showed an open-circuit potential of ca. 600 mV with an impressive fill factor of >0.70, making them attractive candidates for solar energy conversion applications. The visible spectra of the 3,4-toluenedithiol-based sensitizers showed an enhanced red response, but the lower photocurrent efficiency observed for these sensitizers stems in part from a sluggish halide oxidation rate and a fast recombination of injected electrons with the oxidized dye.

1. Introduction

The development of new systems for the conversion of solar light into electrical energy is an important goal. An attractive and cheaper approach has been to utilize large-band-gap oxide semiconductors such as titanium dioxide to absorb solar light.[1] Oxide semiconductors tend to be more stable against photocorrosion than small-band-gap semiconductors such as Si or GaAs.[2] A potential drawback of the oxide semiconductors is their large band gap, which reduces enormously the fraction of solar irradiation that can be harvested. The spectral response can be improved by using a high concentration of dopants. Another attractive possibility is the use of electronically excited states of molecules (sensitizers). Dye sensitization of large-band-gap oxide semiconductors has been investigated for many years.[3] Unfortunately, the light-to-electricity conversion efficiency of conventional dye-sensitized solar cells was previously very low, largely because of either their low light-harvesting efficiency when only a monolayer of dye is adsorbed on a flat-surface electrode or their low charge separation and transfer efficiency when a multilayer dye is adsorbed on a flat-surface electrode.[4] In the 1990s, a major photoelectrochemical solar cell development was accomplished by the introduction of fractal, thin-film, dye-sensitized solar cells devised by Grätzel.[5] A large number of dye molecules with suitable interlocking groups that provide an electronic bridging function between the chromophoric moiety and the conduction band of the semiconductors can be adsorbed onto fractal films, thus allowing an increase in the efficiency of the harvesting of incident visible light.[6] A remarkable feature of fractal films is their ability to collect

* Corresponding authors. Phone: +81-298-61-4641. Fax: +81-298-61-4496. E-mail: sugihara-hideki@aist.go.jp.

(1) Morrison, S. R. *Electrochemistry of Semiconductor and Oxidized Metal Electrodes*; Plenum Press: New York, 1980; and references therein.
(2) Tan, M. X.; Laibinis, P. E.; Nguyen, S. T.; Kesselman, J. M.; Stanton, C. E.; Lewis, N. S. *Prog. Inorg. Chem.* **1994**, *41*, 21.
(3) (a) Meier, H. *J. Phys. Chem.* **1965**, *69*, 724. (b) Gerischer, H. *Photochem. Photobiol.* **1972**, *16*, 243. (c) Tributsch, H.; Calvin, M. *Photochem. Photoboil.* **1971**, *14*, 95. (d) Willing, F.; Gerischer, H. *Top. Curr. Chem.* **1976**, *61*, 31. (e) Miyasaka, T.; Watanabe, T.; Fujishima, A.; Honda, K. *J. Am. Chem. Soc.* **1978**, *100*, 6657. (f) Miyasaka, T.; Watanabe, T.; Fujishima, A.; Honda, K. *Nature* **1979**, *277*, 638. (g) Willing, F. *Chem. Phys. Lett.* **1976**, *40*, 331. (h) Moser, J.; Grätzel, M. *J. Am. Chem. Soc.* **1984**, *106*, 6557. (i) Ryan, M. A.; Fitzgerald, E. C.; Spitler, M. T. *J. Phys. Chem.* **1989**, *93*, 6150. (j) Tsubomura, H.; Matsumura, M.; Nomura, Y.; Amamiya, T. *Nature* **1976**, *261*, 402. (k) Moser, J.; Grätzel, M. *J. Am. Chem. Soc.* **1984**, *106*, 10769.
(4) (a) Nevin, W. A.; Chamberlain, G. A. *J. Appl. Phys.* **1991**, *69*, 4324. (b) Sharma, G. D.; Mathup, S. C.; Dube, D. C. *J. Mater. Sci.* **1991**, *26*, 6547.
(5) O'Regan, B.; Grätzel, M. *Nature* **1991**, *353*, 737.
(6) Vlachopoulos, N.; Liska, P.; Augustynski, J.; Grätzel, M. *J. Am. Chem. Soc.* **1988**, *110*, 1216.

10.1021/ic010391y CCC: $20.00
Published on Web 09/13/2001

photoinjected electrons efficiently throughout a thick, porous semiconducting network.

In this system, a dye molecule absorbs visible light and, after excitation, injects electrons into the conduction band of the semiconductor to produce an electric current. The original state of the dye is subsequently restored by electron donation from a redox system such as the iodide/triiodide couple. There are five key requirements for an efficient sensitizer. (1) Interlocking groups should be present to graft the dye onto the semiconductor surface and to ensure an intimate electronic coupling between the excited-state wave function of the dye and the conduction band manifold of the semiconductor. (2) The absorption of the dye should overlap the solar emission spectrum to allow the maximum power conversion. (3) The excited state should have sufficient thermodynamic driving force to inject electrons into the conduction band. (4) The redox potential should be sufficiently positive to be regenerated via electron donation from the redox electrolyte. (5) The oxidized sensitizer should be sufficiently stable to be quantitatively reduced by an electron.

The photochemistry of transition metal complexes has been thoroughly investigated using polypyridine ligands during the last two decades,[7−12] in part because of their possible applications in light-to-electricity conversion processes. The majority of the work in this area has been on polypyridine complexes of Ru(II) because of their intense charge-transfer (CT) absorptions across the whole visible range, moderately intense emissions with fairly long lifetimes in fluid solutions at ambient temperatures, high quantum yields for the formation of the lowest CT excited state, redox reactivities, and ease of tunability of redox properties.[7] Findings on the photochemistry of ruthenium complexes have also been extended to other charge-transfer complexes such as Os(II),[8] Cu(I),[9] Re(I),[10] Pt(II),[11] Fe(II),[12] and Ir(III).

The most efficient and stable charge-transfer sensitizers employed so far in these solar cells are Ru(II) polypyridyl complexes with carboxylic acid groups bound to nanocrystalline TiO_2 that have been widely studied in the past 10 years.[5,13−18] The photoexcitation of the metal-to-ligand charge-transfer (MLCT) excited states of the adsorbed dye leads to an efficient injection of electrons into the conduction band of the TiO_2. Incident photon-to-current conversion efficiencies (IPCE) exceeding 70% have been reported in several cases.[5,13−15,18] Recently, Lewis and co-workers reported that charge-transfer polypyridyl complexes of Os(II) extended the light absorption and spectral response of nanocrystalline TiO_2 photoelectrodes to longer wavelengths while providing high external quantum yields for photocurrent flow similar to their analogous Ru(II) complexes.[19] Alternative MLCT sensitizers based on Fe(II),[20] Re(I),[21] and Cu(I)[22] have also been employed in solar cells to sensitize nanocrystalline TiO_2 semiconductors, but the solar conversion efficiency is significantly lower than that observed with the Ru(II)- and Os(II)-based sensitizers.

Luminescence from square planar d^8 Pt(II) complexes has been known for many years but is restricted mainly to solid-state or frozen glasses.[23−25] The observation that square planar Pt(II) diimine complexes emit in fluid solution is relatively recent.[26] Most of the solution-emissive complexes that have been reported by Balzani, Scandola, Vogler, Che, and von Zelewsky exhibit a structured emission corresponding to a $^3(\pi-\pi)^*$ intraligand (IL) excited state. These complexes generally absorb

(7) (a) Roundhill, D. M. *Photochemistry and Photophysics of Metal Complexes*; Plenum Press: New York, 1994. (b) Juris, A.; Balzani, V.; Barigelletti, F.; Campagna, S.; Belser, P.; von Zelewsky, A. *Coord. Chem. Rev.* **1988**, *84*, 85. (c) Kalyanasundram, K. *Coord. Chem. Rev.* **1982**, *46*, 159. (d) Meyer, T. J. *Pure Appl. Chem*. **1986**, *58*, 1193. (e) Islam, A.; Ikeda, N.; Nozaki, K.; Ohno, T. *Chem. Phys. Lett*. **1996**, *263*, 209. (f) Islam, A.; Ikeda, N.; Yoshimura, A.; Ohno, T. *Inorg. Chem*. **1998**, *37*, 3093. (g) Islam, A.; Ikeda, N.; Nozaki, K.; Ohno, T. *Photochem. Photobiol*. **1997**, *106*, 61.

(8) (a) Kalyanasundram, K.; Nazeeruddin, M. K. *Chem. Phys. Lett*. **1992**, *193*, 292. (b) Kalyanasundram, K. *Photochemistry of Polypyridine and Porphyrin Complexes*; Academic Press: San Diego, 1992; p 626.

(9) Miller, M. T.; Gantzel, P. K.; Karpishin, T. B. *Inorg. Chem*. **1999**, *38*, 3414.

(10) Sacksteder, L.-A.; Lee, M.; Demas, J. N.; DeGraff, B. A. *J. Am. Chem. Soc.* **1984**, *106*, 6557.

(11) Miskowski, V. M.; Houlding, V. H. *Inorg. Chem*. **1989**, *28*, 1529.

(12) (a) DeLaive, P. J.; Foreman, T. K.; Giannotti, C.; Whitten, D. G. *J. Am. Chem. Soc*. **1980**, *102*, 5627. (b) Winkler, J. R.; Sutin, N. *Inorg. Chem*. **1987**, *26*, 220.

(13) (a) Nazeeruddin, M. K.; Kay, A.; Rodicio, I.; Humphry-Baker, R.; Müller, E.; Liska, P.; Vlachopoulos, N.; Grätzel, M. *J. Am. Chem. Soc*. **1993**, *115*, 6382. (b) Nazeeruddin, M. K.; Péchy, P.; Grätzel, M. *Chem. Commun*. **1997**, 1705. (c) Nazeeruddin, M. K.; Müller, E.; Humphry-Baker, R.; Vlachopoulos, N.; Grätzel, M. *J. Chem. Soc., Dalton Trans.* **1997**, 4571. (d) Ruile, S.; Kohle, O.; Péchy, P.; Grätzel, M. *Inorg. Chim. Acta* **1997**, *261*, 129. (e) Jing, B.; Zhang, H.; Zhang, M.; Lu, Z.; Shen, T. *J. Mater. Chem*. **1998**, *8*, 2055. (f) Moser, J.; Bonnôte, J. E.; Grätzel, M. *Coord. Chem. Rev*. **1998**, *171*, 245. (g) Nazeeruddin, M. K.; Liska, P.; Moser, J.; Vlachopoulos, N.; Grätzel, M. *Helv. Chim. Acta* **1990**, *73*, 1788. (h) Kalyanasundaram, K.; Grätzel, M. *Coord. Chem. Rev*. **1998**, *77*, 347. (i) Ruile, S.; Kohle, O.; Pettersson, H.; Grätzel, M. *New J. Chem*. **1998**, 25. (j) Grätzel, M. *Curr. Opin. Colloid Interface Sci*. **1999**, *4*, 314. (k) Zakeeruddin, S. M.; Nazeeruddin, Md. K.; Humphry-Baker, R.; Grätzel, M.; Shklover, V. *Inorg. Chem*. **1998**, *37*, 5251. (l) Nazeeruddin, Md. K.; Péchy, P.; Renouard, T.; Zakeeruddin, S. M.; Humphry-Baker, R.; Comte, P.; Liska, P.; Cevey, L.; Costa, E.; Shklover, V.; Spiccia, L.; Deacon, G. B.; Bignozzi, C. A.; Grätzel, M. *J. Am. Chem. Soc*. **2001**, *123*, 1613. (m) Nazeeruddin, Md. K.; Zakeeruddin, S. M.; Humphry-Baker, R.; Jirousek, M.; Liska, P.; Vlachopoulos, N.; Shklover, V.; Fischer, C.-H.; Grätzel, M. *Inorg. Chem.* **1999**, *38*, 6298.

(14) (a) Tachibana, Y.; Haque, S. A.; Mercer, I. P.; Durrant, J. R.; Klug, D. R. *J. Phys. Chem. B* **2000**, *104*, 1198. (b) Rehm, J. M.; McLendon, G. L.; Nagasawa, Y.; Yoshihara, K.; Moser, J.; Grätzel, M. *J. Phys. Chem*. **1996**, *100*, 9577. (c) Cherepy, N. J.; Smestad, G. P.; Grätzel, M.; Zhang, J. Z. *J. Phys. Chem. B* **1997**, *101*, 9342.

(15) (a) Sugihara, H.; Singh, L. P.; Sayama, K.; Arakawa, H.; Nazeeruddin, Md. K.; Grätzel, M. *Chem. Lett*. **1998**, 1005. (b) Yanagida, M.; Singh, L. P.; Sayama, K.; Hara, K.; Katoh, R.; Islam, A.; Sugihara, H.; Arakawa, H.; Nazeeruddin, Md. K.; Grätzel, M. *J. Chem. Soc., Dalton Trans.* **2000**, 2817.

(16) Takahashi, Y.; Arakawa, H.; Sugihara, H.; Hara, K.; Islam, A.; Katoh, R.; Tachibana, Y.; Yanagida, M. *Inorg. Chim. Acta* **2000**, *12*, 1083.

(17) (a) Islam, A.; Hara, K.; Singh, L. P.; Katoh, R.; Yanagida, M.; Murata, S.; Takahashi, Y.; Sugihara, H.; Arakawa, H. *Chem. Lett*. **2000**, 490. (b) Islam, A.; Sugihara, H.; Singh, L. P.; Hara, K.; Katoh, R.; Nagawa, Y.; Yanagida, M.; Takahashi, Y.; Murata, S.; Arakawa, H. *Inorg. Chim. Acta* (in press).

(18) Argazzi, R.; Bignozzi, C. A.; Hasselmann, G. M.; Meyer, G. J. *Inorg. Chem*. **1998**, *37*, 4533.

(19) Sauvé, G.; Cass, M. E.; Coia, G.; Doig, S. J.; Lauermann, I.; Pomykal, K. E.; Lewis, N. S. *J. Phys. Chem. B* **2000**, *104*, 6821.

(20) Ferrere, S. *Chem. Mater*. **2000**, *12*, 1083.

(21) Hasselmann, G. M.; Meyer, G. J. *Z. Phys. Chem*. **1999**, *212*, 39.

(22) Alonso-Vante, N.; Nieregarten, J.; Sauvage, J. *J. Chem. Soc., Dalton Trans*. **1994**, 1649.

(23) (a) Webb, D. L.; Rossiello, L. A. *Inorg. Chem*. **1971**, *10*, 2213. (b) Johnson, C. E.; Eisenberg, R.; Evans, T. R.; Burberry, M. S. *J. Am. Chem. Soc*. **1983**, *105*, 1795.

(24) Islam, A.; Okamoto, Y.; Ikeda, N.; Nozaki, K.; Yoshimura, A.; Bovak, G.; Ohno, T. *Coord. Chem. Rev.* **1998**, *171*, 355.

(25) (a) Bailey, J. A.; Hill, M. G.; Marsh, R. E.; Miskowski, V. M.; Schaefer, W. P.; Gray, H. B. *Inorg. Chem*. **1995**, *34*, 4591. (b) Connick, W. B.; Marsh, R. E.; Schaefer, W. P.; Gray, H. B. *Inorg. Chem*. **1997**, *36*, 913.

(26) (a) Ballardini, R.; Varani, G.; Indelli, M. T.; Scandola, F. *Inorg. Chem*. **1986**, *25*, 3858. (b) Sandrini, D.; Maestri, M.; Balzani, V.; Maeder, U.; von Zelewsky, A. *Inorg. Chem*. **1988**, *27*, 2640. (c) Maestri, M.; Sandrini, D.; Balzani, V.; Chassot, L.; Joliet, P.; von Zelewsky, A. *Chem. Phys. Lett.* **1985**, *122*, 375. (d) Sandrini, D.; Maestri, M.; Balzani, V.; Chassot, L.; von Zelewsky, A. *J. Am. Chem. Soc.* **1987**, *109*, 7720. (e) Barigelletti, F.; Sandrini, D.; Maestri, M.; Balzani, V.; von Zelewsky, A.; Chassot, L.; Jolliet, P.; Maeder, U. *Inorg. Chem*. **1988**, *27*, 3644. (f) Che, C.-M.; Wan, K.-T.; He, L.-Y.; Poon, C.-K.; Yam, V. W.-W. *J. Chem. Soc., Chem. Commun.* **1989**, 943. (g) Kunkely, H.; Vogler, A. *J. Am. Chem. Soc.* **1990**, *112*, 5625.

light in the blue and ultraviolet regions. Over the past decade, Eisenberg and co-workers have performed elaborate studies on the charge-transfer excited state of mixed-ligand Pt(II) complexes with diimine and dithiolate ligands.[27−30] For most complexes, the excited state involves a highest occupied molecular orbital (HOMO), which is a mixture of platinum and dithiolate orbital character, and a lowest unoccupied molecular orbital (LUMO), which is a π^* orbital of the diimine and has been termed a "mixed metal-ligand-to-ligand charge-transfer" (MMLL′CT). These complexes have an intense charge-transfer absorption band in the visible region, and the absorption band energies can be tuned throughout the visible range through changes in the electron-donating and -accepting abilities of the diimine and dithiolate ligands.[29] Because the spectra of these complexes have a wide area that overlaps the solar emission spectrum, they are expected to harvest solar light with high efficiency. The CT excited state of these complexes is emissive in fluid solution and undergoes electron-transfer quenching both oxidatively and reductively.[27,29] Thus, square planar Pt(diimine)(dithiolate) complexes have excellent photophysical and electrochemical properties, making them a promising class of charge-transfer sensitizers. In a recent study, we demonstrated that Pt(4,4′-dicarboxy-2,2′-bipyridine)(quinoxaline-2,3-dithiolate) can sensitize nanocrystalline TiO_2 in a dye-sensitized solar-cell device.[31]

In another recent study, we tuned the MLCT transitions up to 600 nm in Ru-diimine sensitizers by using a 4,4′-dicarboxy-2,2′-biquinoline (dcbiq) ligand with a lower π^*-accepting orbital than the commonly utilized 4,4′-dicarboxy-2,2′-bipyridine (dcbpy) ligand.[17] However, the sensitizers did not perform as efficiently as those based on dcbpy or 4,7-dicarboxy-1,10-phenanthroline (dcphen), and the solar light conversion efficiency was decreased largely because of a lower efficiency of electron injection into the conduction band of TiO_2.[5,13a,15] In the present investigation, we utilized different types of 1,1- and 1,2-dithiolates as nonchromophoric chelating ligands with differing electron-donating strengths to tune the sensitizer absorption properties.

We prepared and characterized a series of square planar Pt(NN)(SS)-type sensitizers (**3**−**9**, as shown in Chart 1), where NN is dcbpy or dcphen and SS is one of the four dithiolate ligands: ethyl-2-cyano-3,3-dimercaptoacrylate (ecda), quinoxaline-2,3-dithiolate (qdt), 1,2-benzenedithiolate (bdt), or 3,4-toluenedithiolate (tdt). We tuned the CT-to-diimine excited state by approximately 4000 cm^{-1} using these four dithiolate ligands. The carboxyl groups of the ligand provided grafting functionalities to the TiO_2 surface, ensuring an intimate electronic coupling between the sensitizer and the semiconductor. This paper reports our investigation of the redox and optical properties of these Pt(II)-based sensitizers in fluid solution and the photoelectrochemical behavior on TiO_2. We found that these new Pt(II)-based sensitizers efficiently sensitize TiO_2 beyond 700 nm.

Chart 1

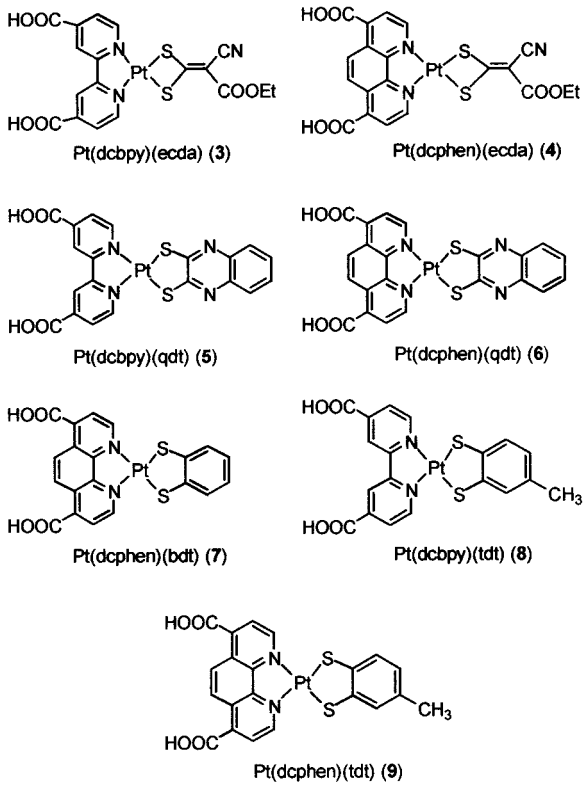

2. Experimental Details

Materials. 1,2-Benzenedithiol (H_2bdt), 3,4-toluenedithiol (H_2tdt), and K_2PtCl_4 were used as received. The 4,4′-dicarboxy-2,2′-bipyridine (dcbpy), 4,7-dicarboxy-1,10-phenanthroline (dcphen),[15] ethyl-2-cyano-3,3-dimercaptoacrylate dipotassium salt (K_2ecda),[32] and quinoxaline-2,3-dithiol (H_2qdt)[33] were prepared according to literature methods.

Synthesis of Pt(dcbpy)Cl_2 (1). A 588 mg (2.41 mmol) sample of dcbpy was slowly dissolved in water (100 mL) by the addition of a 0.1 M KOH solution. The base was added to the suspension in such a way as to keep the pH <8. To this mixture were added 955 mg (2.30 mmol) of K_2PtCl_4 and 600 mg of KCl. After 4 h of refluxing with stirring, the reaction mixture was allowed to cool to room temperature. Pt(dcbpy)Cl_2 was precipitated by the addition of 0.1 M HCl. The light yellow precipitate was filtered off and washed with water. The product was redissolved in a minimal amount of aqueous 0.1 M KOH and purified by column chromatography using Sephadex LH-20 as a column support and water as the eluent. The main yellow band was collected, and the product was precipitated as a neutral complex by the addition of 0.1 M HCl. Compound **1** was isolated by filtration, washed well with H_2O, and dried under vacuum (yield 50%). MS (ESIMS) *m*/*z*: 254.1 $(M - 2H)^{2-}$.

Synthesis of Pt(dcphen)Cl_2 (2). This complex was obtained by a procedure identical to that used for Pt(dcphen)Cl_2 (yield 60%). MS (ESIMS) *m*/*z*: 266.1 $(M - 2H)^{2-}$.

Synthesis of Pt(dcbpy)(ecda) (3). A 510 mg (1 mmol) sample of Pt(dcbpy)Cl_2 was placed in a round-bottom flask containing 50 mL of degassed water and dissolved by a minimal amount of 0.1 M KOH. To this mixture was added a degassed solution of 265 mg (1 mmol) of K_2ecda in 15 mL of MeOH. A bright yellow solution formed immediately and was stirred for an additional 2 h. The product was

(27) (a) Zuleta, J. A.; Burberry, M. S.; Eisenberg, R. *Coord. Chem. Rev.* **1990**, *97*, 47. (b) Paw, W.; Cummings, S. D.; Mansour, M. A.; Connick, W. B.; Geiger, D. K.; Eisenberg, R. *Coord. Chem. Rev.* **1998**, *171*, 125.
(28) (a) Cummings, S. D.; Eisenberg, R. *Inorg. Chem.* **1995**, *34*, 2007. (b) Cummings, S. D.; Eisenberg, R. *Inorg. Chem.* **1995**, *34*, 3396.
(29) Cummings, S. D.; Eisenberg, R. *J. Am. Chem. Soc.* **1996**, *118*, 1949.
(30) (a) Bevilacqua, J. M.; Eisenberg, R. *Inorg. Chem.* **1994**, *33*, 2913. (b) Zuleta, J. A.; Bevilacqua, J. M.; Proserpio, D. M.; Harvey, P. D.; Eisenberg, R. *Inorg. Chem.* **1992**, *31*, 2396. (c) Zuleta, J. A.; Bevilacqua, J. M.; Rehm, J. M.; Eisenberg, R. *Inorg. Chem.* **1992**, *31*, 1332. (d) Bevilacqua, J. M.; Eisenberg, R. *Inorg. Chem.* **1994**, *33*, 1886. (e) Cummings, S. D.; Cheng, L. T.; Eisenberg, R. *Chem. Mater.* **1997**, *9*, 440.
(31) Islam, A.; Sugihara, H.; Hara, K.; Singh, L. P.; Katoh, R.; Yanagida, M.; Takahashi, Y.; Murata, S.; Arakawa, H. *New J. Chem.* **2000**, *24*, 343.
(32) Jensen, K. A.; Henriksen, L. *Acta Chem. Scand.* **1968**, *22*, 1107.
(33) Theriot, L. J.; Ganguli, K. K.; Kavarnos, S.; Bernal, I. *J. Inorg. Nucl. Chem.* **1969**, *31*, 3133.

precipitated by adding 0.1 M HCl and filtered off. Purification was carried out on a Sephadex LH-20 column with water as the eluent. The bright yellow band was collected, and the solvent volume was reduced to 10 mL. The addition of a few drops of 0.1 M HCl resulted in the precipitation of a yellow powder, which was collected by filtration, washed several times with water, and dried under vacuum (yield 65%). MS (ESIMS) *m*/*z*: 311.7 $(M - 2H)^{2-}$, 646.9 $(M - 2H + Na)^{-}$. ^{1}H NMR (300 MHz, D_2O-NaOD): δ 8.76 (H, d), 8.39 (H, s), 7.84 (H, d), 7.76 (H, d), 7.54 (H, s), 7.50 (H, d), 4.02 (2H, d), 1.22 (3H, t). Anal. Calcd for $C_{18}H_{13}N_3O_6S_2Pt\cdot CH_3OH$: C, 34.65; H, 2.60; N, 6.38; S, 9.74. Found: C, 35.28; H, 2.51; N, 6.65; S, 9.20.

Synthesis of Pt(dcphen)(ecda) (4). The complex was prepared using a procedure analogous to that used for Pt(dcbpy)(ecda) using Pt(dcphen)Cl_2 and K_2ecda. MS (ESIMS) *m*/*z*: 323.6 $(M - 2H)^{2-}$, 650.4 $(M - H)^{-}$, 686.6 $(M - 2H + K)^{-}$. ^{1}H NMR (300 MHz, D_2O-NaOD): δ 8.38 (2H, s), 8.08 (2H, d), 7.72 (2H, d), 4.02 (2H, d), 1.22 (3H, t). Anal. Calcd for $C_{20}H_{13}N_3O_6S_2Pt\cdot H_2O$: C, 35.93; H, 2.26; N, 6.29; S, 9.59. Found: C, 35.55; H, 2.22; N, 6.02; S, 9.20.

Synthesis of Pt(dcbpy)(qdt) (5). The complex was prepared by a procedure analogous to that for Pt(dcbpy)(ecda) described above, using 510 mg (1 mmol) of Pt(dcbpy)Cl_2 and 193 mg (1 mmol) of H_2qdt. The red-orange precipitate obtained after column purification was dissolved in 10 mL of a 10% tetrabutylammonium hydroxide (TBAOH) aqueous solution. This solution was adjusted to pH 4 by the addition of 0.1 M HCl and kept in a refrigerator overnight. The deep orange precipitate was collected on a membrane filter (yield 65%). MS (ESIMS) *m*/*z*: 314.1 $(M - 2H)^{2-}$, 629.7 $(M - H)^{-}$, 651.3 $(M - H + Na)^{-}$. ^{1}H NMR (300 MHz, D_2O-NaOD): δ 8.76 (H, d), 8.38 (H, s), 8.00 (H, d), 7.84 (H, d), 7.54 (H, q), 7.41 (2H, st), 7.17 (H, d), 7.10 (H, q), 6.91 (H, t). Anal. Calcd for $C_{20}H_{11}N_4O_4S_2Pt\cdot TBA$: C, 49.53; H, 5.43; N, 8.02; S, 7.35. Found: C, 49.14; H, 5.35; N, 8.20; S, 7.70.

Synthesis of Pt(dcphen)(qdt) (6). The complex was prepared using a procedure analogous to that used for Pt(dcbpy)(qdt) using Pt(dcphen)Cl_2 and H_2qdt. MS (ESIMS) *m*/*z*: 326.7 $(M - 2H)^{2-}$, 691.6 $(M - H + K)^{-}$. ^{1}H NMR (300 MHz, D_2O-NaOD): δ 8.68 (2H, d), 7.84 (2H, d), 7.68 (2H, s), 6.69 (2H, q), 6.56 (2H, t). Anal. Calcd for $C_{22}H_{10}N_4O_4S_2Pt\cdot(TBA)_2(H_2O)_2$: C, 55.22; H, 7.38; N, 7.17; S, 5.46. Found: C, 55.79; H, 7.77; N, 6.98; S, 4.86.

Synthesis of Pt(dcphen)(bdt) (7). The complex was prepared using a procedure analogous to that used for Pt(dcbpy)(ecda) using Pt(dcphen)Cl_2 and H_2bdt. MS (ESIMS) *m*/*z*: 300.7 $(M - 2H)^{2-}$, 602.7 $(M - H)^{-}$. ^{1}H NMR (300 MHz, D_2O-NaOD): δ 9.07 (2H, d), 8.04 (2H, s), 8.02 (2H, d), 7.02 (2H, dd), 6.86 (2H, tt). Anal. Calcd for $C_{20}H_{12}N_2O_4S_2Pt\cdot\times H_2O$: C, 38.65; H, 2.27; N, 4.51; S, 10.32. Found: C, 38.68; H, 2.44; N, 4.41; S, 10.11.

Synthesis of Pt(dcbpy)(tdt) (8). The complex was prepared using the same procedure as that for Pt(dcbpy)(ecda) described above, except H_2tdt was used in place of K_2ecda. MS (ESIMS) *m*/*z*: 295.3 $(M - 2H)^{2-}$, 591.8 $(M - H)^{-}$, 613.8 $(M - 2H + Na)^{-}$. ^{1}H NMR (300 MHz, D_2O-NaOD): δ 8.68 (2H, t), 8.16 (2H, d), 7.65 (2H, tt), 6.80 (1H, d), 6.71 (1H, s), 6.56 (1H, d), 2.22 (3H, s). Anal. Calcd for $C_{19}H_{14}N_2O_4S_2Pt\cdot H_2O$: C, 37.75; H, 2.44; N, 4.53; S, 10.49. Found: C, 37.32; H, 2.64; N, 4.58; S, 10.47.

Synthesis of Pt(dcphen)(tdt) (9). The complex was prepared using a procedure analogous to that used for Pt(dcbpy)(ecda) using Pt(dcphen)Cl_2 and H_2tdt. MS (ESIMS) *m*/*z*: 307.4 $(M - 2H)^{2-}$, 615.7 $(M - H)^{-}$, 653.6 $(M - 2H + Na)^{-}$. ^{1}H NMR (300 MHz, D_2O-NaOD): δ 9.05 (2H, t), 7.98 (2H, t), 7.93 (2H, s), 6.73 (1H, d), 6.62 (1H, s), 6.56 (1H, d), 2.23 (3H, s). Anal. Calcd for $C_{21}H_{14}N_2O_4S_2Pt\cdot H_2O$: C, 39.72; H, 2.43; N, 4.28; S, 9.70. Found: C, 39.68; H, 2.54; N, 4.39; S, 10.01.

Analytical Measurements. Spectroscopic Studies. UV−vis and fluorescence spectra were recorded on a Shimadzu UV-3101PC spectrophotometer and a Hitachi F-4500 spectrophotometer, respectively. Spectrophotometric titrations were performed in a 1×10^{-5} M, 9:1 H_2O/ethanol solution containing 0.1 M LiCl. The initial pH was adjusted to 10.5 by adding 0.2 M NaOH. The UV−vis spectrum of each solution was obtained after adding aliquots of 0.2 M HNO_3 and allowing the solution to equilibrate for 5 min. The measured emission spectra were corrected for wavelength-dependent features. Spectra at 77 K were obtained by cooling the samples in a quartz Dewar flask filled with liquid nitrogen. The emission lifetimes were measured by exciting the sample with a ~7 ns pulse at 500 nm from an optical parametric oscillator (Surelite OPO) pumped at 355 nm by an Nd:YAG laser (Continum Surelite II). A Hamamatsu R928 photomultiplier was used to convert the light signal to a voltage signal, and the emission decay was followed on a Tektronix TDS680C digitizing signal analyzer. ^{1}H NMR spectra were recorded with a Varian 300BB spectrometer. Electron spray ionization mass spectra (ESIMS) were obtained on a Micromass Quattro II mass spectrometer. A BET experiment was performed with an automatic surface-area analyzer (GEMINI 2360).

Emission Spectral Fitting. For emission spectral fitting, a two-mode Franck−Condon analysis of the emission spectra was used.[34] Equation 1,

$$I(\bar{\nu}) = \left(\frac{\bar{\nu}}{\bar{\nu}_{0-0}}\right)^3 \sum_{n_M=0}\sum_{n_L=0} \exp(-S_M - S_L)\frac{S_M^{n_M}}{n_M!}\frac{S_L^{n_L}}{n_L!}\sqrt{\frac{4\ln 2}{\pi\Delta\bar{\nu}_{1/2}^2}} \exp\left[-\frac{4\ln 2(\bar{\nu} - \bar{\nu}_{0-0} + n_M\bar{\nu}_M + n_L\bar{\nu}_L)^2}{\Delta\bar{\nu}_{1/2}^2}\right] \quad (1)$$

was used to calculate the best fit, where $I(\nu)$ is the relative emitted light intensity at a certain energy (in wavenumbers), n_M and n_L are the vibrational quantum numbers of accepting vibrational modes of medium (ν_M) and low (ν_L) frequencies, respectively, S_M and S_L are the electronic-vibrational coupling constants, or Huang−Rhys factors, which are related to the displacement along the molecular coordinates corresponding to the medium-frequency and low-frequency acceptor modes, respectively, ν_{0-0} is the energy difference between the excited and ground states in the lowest vibrational levels, and $\Delta\nu_{1/2}$ is the full width at half-maximum (fwhm) of the vibronic lines of the emission and increases with the square root of the temperature. ν_M is obtained from the spectral fits ($\nu_M \approx 1300$ cm^{-1}) and is near the observed spacing in the 77 K emission spectra, and ν_L is taken as a typical metal−ligand stretching frequency ($\nu_L = 370$ cm^{-1}). To obtain the best fit of the observed spectra, the values of S_M, S_L, $\Delta\nu_{1/2}$, and ν_{0-0} were varied.

Electrochemistry. The redox potentials of the complexes were measured using a standard three-electrode apparatus comprised of a platinum wire counter electrode, a carbon or platinum disk working electrode, and an Ag/AgCl (saturated aqueous KCl) reference electrode in contact with a KCl salt bridge. Cyclic voltammograms were collected using a BAS-100 electrochemical analyzer (Bioanalytical Systems). Methanol was used as a solvent, and the supporting electrolyte was 0.1 M tetrabutylammonium perchlorate. Electrode potential values were corrected to the saturated calomel electrode (SCE).

Preparation of Thin-Layer Films. Nanoporous TiO_2 semiconductor thin films approximately 16 μm thick on SnO_2-coated glass were prepared using a previously published procedure.[35] The thin films were coated for 15 h at room temperature in a 5×10^{-5} M ethanolic dye solution containing 30 mmol of deoxycholic acid as a coadsorbate. The amount of adsorbed dye was determined by desorbing the dye from the oxide semiconductor films into a solution of 1×10^{-4} M NaOH in H_2O and measuring its absorption spectrum.

Photoelectrochemical Measurements. Photoelectrochemical measurements were performed in a two-electrode sandwich cell configuration as previously reported.[36] A mixture containing 0.6 M 1,2-dimethyl-3-propylimidazolium iodide (DMPII), 50 mM I_2, 0.5 M 4-*tert*-butylpyridine (TBP), and 0.1 M LiI in acetonitrile was used as the electrolyte. The working electrode was illuminated through a conducting glass, and the illuminated surface area was 0.25 or 1.0 cm^2.

The photocurrent and photovoltage were measured under simulated solar light (Wacom Co., WXS-80C-3, AM 1.5, 100 mW/cm^2) using a potentiostat with a nonresistance ammeter (Nikko Keisoku Co., NPGS-2501). Monochromatic illumination was obtained using a 500 W halogen lamp (Ushio Denki Co.) in combination with a grating

(34) Anderson, S.; Constable, E. C.; Seddon, K. R.; Turp, J. E.; Baggott, J. E.; Pilling, M. J. *J. Chem. Soc., Dalton Trans.* **1985**, 2247.
(35) Hara, K.; Horiguchi, T.; Kinoshita, T.; Sayama, K.; Sugihara, H.; Arakawa, H. *Sol. Energy Mater. Sol. Cells* **2000**, *64*, 115.
(36) Sayama, K.; Sugihara, H.; Arakawa, H. *Chem. Mater.* **1998**, *10*, 3825.

Table 1. Absorption and Luminescence Properties of the Pt(diimine)(dithiolate) Sensitizers[a]

sensitizer	absorption,[b] λ_{max}(nm) (ϵ (10^3 M^{-1} cm^{-1}))			emission			
				λ_{max}[c] (nm)		τ (μs)	
				298 K	77 K	298 K	77 K
3 Pt(dcbpy)(ecda)	242 (27.4), 306 (19.9)	343 (28.4)	440 (13.0)	641	563	0.02	8.6
4 Pt(dcphen)(ecda)	275 (32.5)	341 (24.9)	436 (14.0)	595	549	0.01	9.3
5 Pt(dcbpy)(qdt)	254 (27.7), 305[d] (13.4)	425 (11.4), 460 (10.3)	495[d] (5.3)	654	565	0.06	50.0
6 Pt(dcphen)(qdt)	267 (34.9)	396 (11.2), 420 (13.1)	480 (15.3)	640	567	0.16	53.0
7 Pt(dcphen)(bdt)	255 (27.0), 279 (24.9)	411 (2.3)	565 (5.2)	780	725	0.19	4.0
8 Pt(dcbpy)(tdt)	253 (27.9), 316 (15.5)	365[d] (2.33)	580 (4.0)	795	735	0.19	3.7
9 Pt(dcphen)(tdt)	256 (29.6), 280 (31)	402[d] (4.32), 477 (5.8)	568 (5.7)	790	730	0.08	1.2

[a] Absorption and luminescence properties of the sensitizers measured in a basic 4:1 ethanol/methanol solution. [b] Absorption maximum, ±2 nm. [c] Emission maximum, ±4 nm. [d] Appeared as a shoulder.

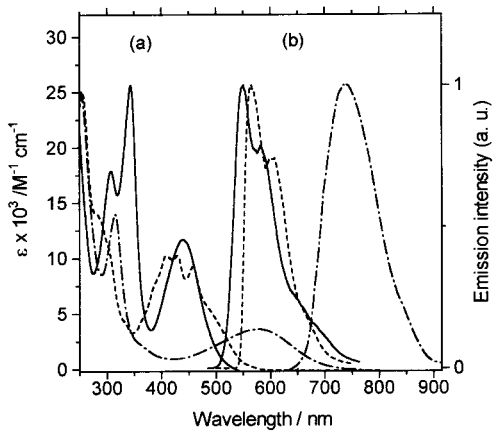

Figure 1. Absorption and emission spectra of Pt(dcbpy)(ecda) (—), Pt(dcbpy)(qdt) (– – –), and Pt(dcbpy)(tdt) (– · –) in a 4:1 ethanol/methanol solution: (a) absorption spectra at 298 K and (b) emission spectra at 77 K.

monochromator model (Jasco, CT-10), a scanning controller (Jasco, SMD-25C), and a multimeter (Keithley, 2000). The light intensities of the monochromatic and solar-simulated light were estimated with an optical power meter (Advantest, TQ8210) and a thermopile (The Eppley Laboratory, Inc.; Newport, RI), respectively.

Incident photon-to-current conversion efficiencies (IPCE) at each incident wavelength were calculated from[13a]

$$\mathrm{IPCE}(\%) = \frac{(1250\ \mathrm{eV\ nm})I_{ph}}{\lambda P_0} \times 100 \qquad (2)$$

where I_{ph} is the photocurrent density at short circuit (μA/cm^2), λ is the wavelength of incident radiation (nm), and P_0 is the photon flux (μW/cm^2). The light-harvesting efficiency (LHE), which is the percent of the light absorbed by the adsorbed chromophores, is given by

$$\mathrm{LHE}(\lambda) = 1 - 10^{-(1000\epsilon\Gamma)} \qquad (3)$$

where Γ is the surface coverage (mol/cm^2) and ϵ is the dye molar absorption coefficient (mol^{-1} cm^{-1}) at a wavelength λ.

3. Results and Discussion

3.1. Electronic Absorption Spectra. The Pt(diimine)(dithiolate) complexes (**3**−**9**, as shown in Chart 1) investigated in this study were characterized by electronic, mass, and ^{1}H NMR spectroscopies and were found to be analytically pure. All are stable over long periods of time in air and light. The absorption and luminescence spectral properties of the investigated complexes are summarized in Table 1. Absorption maxima are listed for the intense low-energy bands in ethanol/methanol, although the spectra possess additional absorption features at higher energies. Figure 1 shows typical absorption and emission spectra of complexes Pt(dcbpy)(ecda), Pt(dcbpy)(qdt), and Pt(dcbpy)(tdt) in an ethanol/methanol solution. All of these Pt(II) complexes showed solvent-insensitive, intense UV bands at 242−316 nm and were assigned to the intraligand $\pi-\pi^*$ transition of the 4,4′-dicarboxy-2,2′-bipyridine or 4,7-dicarboxy-1,10-phenanthroline ligand.[29] Upon acidification, these bands shifted to longer wavelengths because of protonation of the carboxylate groups. All the Pt(diimine)(dithiolate) complexes exhibited a broad band in the 400−600 nm range of their respective absorption spectra in an ethanol/methanol solution, with a molar extinction coefficient of 4000−15000 M^{-1} cm^{-1} (Figure 1a). The positions of the lowest-energy absorption maxima were shifted to higher energies in water, which is a more polar solvent (Table 2). The lower-energy absorption band of Pt(dcbpy)(qdt) shifted from 510 nm in DMF to 440 nm in water. This blue shift indicates a polar ground state and a nonpolar excited state. On the basis of spectroscopic changes that result from systematic chelating ligand modification, a strong solvatochromic shift of the low-energy feature, and molecular orbital calculations of similar types of Pt(II) diimine dithiolate complexes, Eisenberg and co-workers assigned these low-energy transitions as mixed-Pt/dithiolate-to-diimine charge transfers.[27−29] For all the Pt(diimine)(dithiolate) complexes investigated here, a similar assignment of charge-transfer transition holds, involving a transition from a highest occupied molecular orbital (HOMO), which has a mixture of platinum and dithiolate orbital character, to a lowest unoccupied molecular orbital (LUMO), which is a low-energy π^* orbital of the dcbpy or dcphen ligand.

Table 2. Charge-Transfer Absorption Band Maxima of the Pt(diimine)(dithiolate) Sensitizers

sensitizer	absorption,[a] λ_{max} (nm)		
	in H_2O	in EtOH/MeOH[b]	on TiO_2[c]
Pt(dcbpy)(ecda)	402	440	470
Pt(dcphen)(ecda)	407	436	440
Pt(dcbpy)(qdt)	440	495[d]	515
Pt(dcphen)(qdt)	444	480	513
Pt(dcphen)(bdt)	490	565	590
Pt(dcbpy)(tdt)	514	580	600
Pt(dcphen)(tdt)	500	568	595

[a] Absorption maximum, ±2 nm. [b] Measured in a basic 4:1 ethanol/methanol solution. [c] TiO_2 film background has been subtracted. [d] Appeared as a shoulder.

Upon adsorption onto TiO_2, the visible bands in the absorption spectra become broader and red shifted compared to the corresponding absorption bands observed in aqueous and ethanolic solutions (Table 2). This peak energy shift, which is observed for many Ru-based complexes,[13] may be due to the change in the energy levels of the ground and excited states caused by adsorption, which results from the interactions between the dye and the substrate.

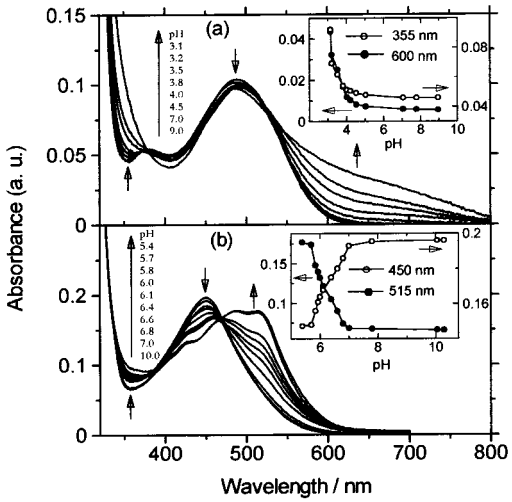

Figure 2. (a) Absorption spectral changes of Pt(dcphen)(bdt) as a function of pH, measured at a concentration of 1.0×10^{-5} M. The inset shows absorbance vs pH at 355 and 600 nm. (b) Absorption spectral changes of Pt(dcbpy)(qdt) as a function of pH, measured at a concentration of 1.2×10^{-5} M. The inset shows absorbance vs pH at 450 and 515 nm.

3.2. pH-Dependent Absorption. The investigated complexes exhibit pH-sensitive electronic spectra. These effects were investigated in spectrophotometric titrations of Pt(dcphen)(bdt) and Pt(dcbpy)(qdt) in 9:1 H_2O/ethanol. Figure 2 shows the absorption change upon addition of acid to alkaline solutions of Pt(dcphen)(bdt) and Pt(dcbpy)(qdt). In the former, as the pH of the solution was lowered from 9 to 3, the absorbance of the lowest-energy absorption band at 490 nm decreased while absorbance increased in the 600 nm region (Figure 2a). A set of isosbestic points at 378 and 525 nm confirmed the presence of only two absorbing species in the solution. Titration curves, obtained by plotting the absorbance change at 355 and 600 nm against pH, showed a clear inflection point at pH 3.2, giving a pK_a value of 3.2 ± 0.1. We assigned this to the proton dissociation of the carboxylic groups of the dcphen ligand. The pronounced increase of absorbance in the 650 nm region upon protonation of the carboxylate anion is due to the stronger electron-withdrawing nature of the COOH groups compared to that of the COO^- anions, which stabilized the energy of the π^* orbital of the dcphen ligand, resulting in a red shift of the CT-to-dcphen transition. This value is similar to the first pK_a values observed for ruthenium complexes of 4,4′-dicarboxy-2,2′-bipyridine[13c] and 4,7-dicarboxy-1,10-phenanthroline (dcphen)[15] ligands. Nazeeruddin and co-workers investigated the Ru(dcbpy)$_2$(NCS)$_2$ complex and found that the dissociation of protons occurs in two steps (pK_a = 3 and 1.5).[13m] We could not observe the second protonation at the carboxylate group of the dcphen ligand because the complex precipitated below pH 3.0.

When acid was added to the Pt(dcbpy)(qdt) solution, changes in the electronic spectrum occurred as shown in Figure 2b. As the solution pH was lowered from 11 to 5, the decrease in the absorbance band at 450 nm was accompanied by the emergence of a new broad feature with a maximum at 515 nm and an increase in absorbance in the 358 nm region. Throughout the titration, clean isosbestic points were maintained at 330, 386, and 469 nm, indicating the presence of only two absorbing species in the solution. Titration curves, obtained by plotting the absorbance change at 450 and 515 nm against pH, showed a clear inflection point at a pH of 6.2, giving the ground-state pK_a value of 6.2 ± 0.1. We assigned this to the protonation of the imine nitrogen of the qdt ligand. These values are larger than the pK_a (≈5) observed for the neutral complex Pt(phen)(qdt).[28b] This is almost certainly a result of the neutral charge of Pt(phen)(qdt) compared to the dianionic charge of Pt(dcbpy)(qdt)$^{2-}$. The observed changes in absorption spectra upon addition of acid suggest that both the charge-transfer to diimine and charge-transfer to dithiolate transitions in fully deprotonated Pt(dcbpy)(qdt)$^{2-}$ are close to each other. Upon protonation of the qdt N atom, the π^* orbital of the qdt ligand is lowered in energy relative to the dcbpy π^* orbital, which lowers the energy of the CT-to-qdt state as well. Since the π^* qdt orbital is not involved directly in the CT-to-dcbpy transition, protonation of the qdt ligand is expected to lead to only a small change in this transition. This is consistent with the observed red shift of the low-energy CT band upon protonation of Pt(dcbpy)(qdt). The molecular orbital calculation for Pt(bpy)(mnt), where mnt is maleonitriledithiolate, shows that the LUMO is a π^* (diimine) orbital, and the π^* (mnt) level is immediately above the LUMO.[30b] We could not determine the pK_a values of the protonation of the carboxylate groups of this complex because the complex precipitated below pH 5.

3.3. Electronic Emission Spectra. All the Pt(diimine)(dithiolate) complexes in a degassed ethanol/methanol solution at 298 K exhibited a luminescence consisting of a single broad band with a maximum between 595 and 795 nm. In frozen ethanol/methanol solutions at 77 K, the emission profiles shifted to higher energies, displaying an increased degree of structure, with well-defined features having an energy separation of ca. 1300 cm^{-1}. The emission spectra of Pt(dcbpy)(ecda), Pt(dcbpy)(qdt), and Pt(dcbpy)(tdt) in an ethanol/methanol glass matrix at 77 K are presented in Figure 1b. The emission energy maxima and lifetime for ethanol/methanol fluid solution and frozen glass solution samples, respectively, of each complex are included in Table 1. The blue shift that occurs for all of the complexes in going from fluid solution to frozen solvent glass is a common rigidochromic effect observed for many metal diimine complexes.[7b,f] All the complexes displayed excited-state lifetimes ranging from 1.2 to 53 μs at 77 K. The lifetimes decreased significantly with increasing temperature, becoming 10−190 ns in fluid solution at 298 K. The very short-lived excited state in fluid solution may be caused by efficient nonradiative decay via low-lying ligand field excited states or solvent interactions in the open coordination sites.[25]

To obtain information about the energy difference between the lowest excited state and the ground state, we analyzed the emission spectra of Pt(dcbpy)(ecda), Pt(dcphen)(ecda), Pt(dcbpy)(qdt), and Pt(dcphen)(qdt) in terms of the two-mode Franck−Condon method (eq 1). The 77 K emission spectra were fitted by using medium-frequency ($\nu_M \approx 1300$ cm^{-1}) and low-frequency ($\nu_L = 370$ cm^{-1}) acceptor modes. The medium-frequency mode was allowed to vary to give a best fit of the observed vibrational progression in the 77 K emission spectra (Figure 1). The low-frequency mode was fixed because there was insufficient resolution in the spectra to determine it accurately. Good fits for the 77 K spectra could be obtained by these means because there was sufficient spectral resolution to define the floating parameters independently. The values of the 77 K spectral-fitting parameters, S_M, S_L, $\Delta\nu_{1/2}$, and ν_{0-0}, of complexes Pt(dcbpy)(ecda), Pt(dcphen)(ecda), Pt(dcbpy)(qdt), and Pt(dcphen)(qdt) are shown in Table 3. The room-temperature emission spectra of these complexes were also simulated by using the same values of ν_M, ν_L, S_M, and S_L obtained from the 77 K emission spectral fitting of a complex; only the values of ν_{0-0} and $\Delta\nu_{1/2}$ were varied to obtain a fit. In the estimation

Table 3. Emission Spectral-Fitting Parameters and Electrochemical Properties of the Pt(diimine)(dithiolate) Sensitizers

sensitizer	emission[a] ν_{max} (cm^{-1})	ν_{0-0}[b] (cm^{-1} (eV))	S_M[b]	S_L[b]	$\Delta\nu_{1/2}$[b] (cm^{-1})	$E(Pt^{3+/2+})$[c] vs SCE	$E(Pt^{1+/2+})$[c] vs SCE	$E^*(Pt^{3+/2+})$[d] vs SCE
Pt(dcbpy)(ecda)	17 760	18 200 (2.25)	0.79	1.77	725	+0.95	−1.1	−1.30
Pt(dcphen)(ecda)	18 200	18 590 (2.30)	0.80	1.88	695	+0.98	−1.2	−1.32
Pt(dcbpy)(qdt)	17 700	18 050 (2.24)	0.82	1.62	725	+0.85	−1.1	−1.39
Pt(dcphen)(qdt)	17 640	17 920 (2.22)	0.66	1.40	560	+0.90	−1.0	−1.32
Pt(dcphen)(bdt)	13 790	14 800 (1.84)[e]				+0.52	−1.1	−1.32
Pt(dcbpy)(tdt)	13 610	14 500 (1.80)[e]				+0.45	−1.2	−1.35
Pt(dcphen)(tdt)	13 700	14 700 (1.82)[e]				+0.49	−1.2	−1.33

[a] Maximum of the corrected emission at 77 K in a deaerated 4:1 EtOH/MeOH solution. [b] ν_{0-0} is the energy difference between the excited and ground states in the lowest vibrational levels, $\Delta\nu_{1/2}$ is the fwhm of the vibronic lines of the emission, and S_M and S_L are the electronic-vibrational coupling constants. All parameters were obtained from a spectral fitting of the emission spectrum at 77 K using eq 1. [c] Irreversible process, anodic peak potential given. [d] Calculated from eq 4. [e] ν_{0-0} values were estimated from the crossing point of the emission and absorption spectra (both in EtOH/MeOH) when the most intense MLCT absorption band and the emission peak were adjusted to the same height.

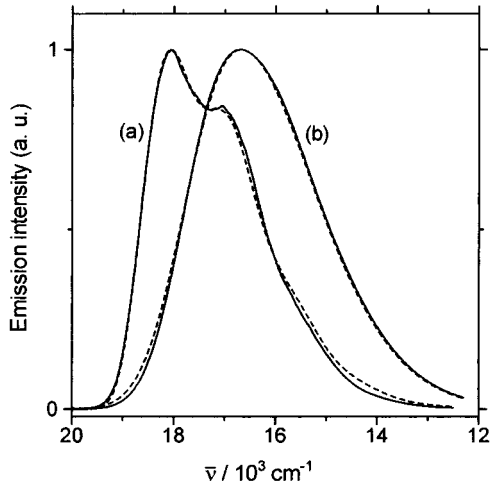

Figure 3. Analysis of the emission spectra of Pt(dcphen)(ecda) in 4:1 ethanol/methanol at 77 K (a) and 298 K (b) in accordance with eq 1. The solid lines represent the experimental spectra; the dashed lines are the spectra calculated using the fitting parameters $\nu_{0-0} = 18\ 590\ cm^{-1}$, $\Delta\nu_{1/2} = 695\ cm^{-1}$, $\nu_M = 1305\ cm^{-1}$, $\nu_L = 370\ cm^{-1}$, $S_M = 0.80$, and $S_L = 1.88$ for the 77 K spectrum (a) and $\nu_{0-0} = 17\ 580\ cm^{-1}$, $\Delta\nu_{1/2} = 1410\ cm^{-1}$, $\nu_M = 1300\ cm^{-1}$, $\nu_L = 370\ cm^{-1}$, $S_M = 0.85$, and $S_L = 1.80$ for the 298 K spectrum (b).

of $\Delta\nu_{1/2}$ from the 77 K spectra, the predicted linear dependence of $\Delta\nu_{1/2}$ on $T^{1/2}$ must be included.[37] In comparing the 77 K spectra to room-temperature spectra, we found that the values of ν_{0-0} obtained in the fits typically shifted 1000−1500 cm^{-1} to lower energies. The shift may be caused by the rotation of the solvent molecules at room temperature, which minimizes the excited-state energy. It should be noted that because of the lack of spectral resolution, ν_{0-0} could not be rigorously determined. A representative example of such a fit is illustrated in Figure 3 for Pt(dcphen)(ecda). We were unable to fit the emission spectra of the bdt and tdt complexes because of the lack of spectral resolution, so ν_{0-0} values were estimated from the crossing point of the 77 K emission and room-temperature absorption spectra when the most intense MLCT absorption band and the emission peak were adjusted to the same height. Table 3 shows that the nature of the dithiolate ligands markedly influences the ν_{0-0} energy. The ν_{0-0} energies decrease along the series ecda > qdt > bdt > tdt.

3.4. Electrochemical Properties. As a means of examining the HOMO and LUMO of the complexes, we obtained cyclic voltammograms. The ground-state redox potentials of all the complexes are summarized in Table 3. All the complexes exhibit an irreversible oxidation wave for the $Pt^{3+/2+}$ couple ranging from +0.98 to +0.45 V vs SCE and an irreversible reduction wave for the $Pt^{2+/1+}$ couple ranging from −1.0 to −1.2 V vs SCE. The formation of a CT-to-diimine excited state formally involves the oxidation of a HOMO having dithiolate and metal orbital character and the reduction of a diimine-based LUMO. The ground-state redox potentials listed in Table 3 display the following general trend: diimine influences the reduction potentials, whereas dithiolate influences the oxidation potentials. For the investigated complexes, the energy of the acceptor orbital (LUMO) remains nearly constant and the decrease in transition energy (e.g., ν_{0-0}) arises mainly from an increase in the energy of the donor orbital (HOMO).

The excited-state oxidation potential, $E^*(Pt^{3+/2+})$, measures the ease of losing the electron that is placed in the π^* orbital of the dcbpy or dcphen ligand upon excitation. For all the studied Pt(diimine)(dithiolate) complexes, $E^*(Pt^{3+/2+})$ values were estimated by

$$E^*(Pt^{3+/2+}) = E(Pt^{3+/2+}) - \nu_{0-0}(eV) \qquad (4)$$

where $E(Pt^{3+/2+})$ is the oxidation potential of the ground state and ν_{0-0} is the energy difference between the excited and ground states. The values of ν_{0-0} were estimated from the spectral fitting of the 77 K emission given in Table 3. The use of eq 4 ignores differences in the oxidation potentials of the free dye and the dye at the surface of the TiO_2. The resulting $E^*(Pt^{3+/2+})$ values are shown in Table 3. All the complexes possess a small range of $E^*(Pt^{3+/2+})$ values (−1.39 to −1.30 V vs SCE), which is consistent with a diimine-localized LUMO. The excited states of all the complexes lie above the conduction band edge (−0.82 V vs SCE) of the nanocrystalline TiO_2 semiconductor.[38] Therefore, an efficient electron injection into the conduction band of the TiO_2 is expected for all these sensitizers (**3**−**9**, as shown in Chart 1).

3.5. Tuning the Excited-State Energy. A key requirement for an efficient sensitizer is that the dye absorption overlap the solar emission spectrum so to allow maximum power conversion. The mixed-Pt/dithiolate-to-diimine charge-transfer transitions of the Pt(diimine)(dithiolate) complexes can be tuned in two ways: (1) by introducing a diimine ligand with a low-lying π^* molecular orbital (LUMO) or (2) by destabilizing the HOMO by increasing the donor properties of the dithiolate ligand. In this study, we tuned the excited-state energies of the Pt(diimine)-(dithiolate) complexes by approximately 4000 cm^{-1} by the variation of the dithiolate ligands having different electron-donating strengths (Table 3). The CT absorption band maxima

(37) Ballhausen, C. J. *Molecular Electronic Structures of Transition Metal Complexes*; McGraw-Hill: New York, 1979.

(38) Hagfeld, A.; Grätzel, M. *Chem. Rev.* **1995**, *95*, 49.

Table 4. Photoelectrochemical Properties of Pt(diimine)(dithiolate) Sensitizers[a]

sensitizer	$\Gamma \times 10^{-7}$ [b] (mol/cm^2)	LHE[c]	IPCE$_{max}$[d]	J_{SC} (mA/cm^2)	J_{SC}[e] (mA/cm^2)	V_{oc} (mV)	V_{oc}[e] (mV)	ff	η (%)
Pt(dcbpy)(ecda)	1.4	0.98	38	2.92	4.28	521	445	0.72	1.10
Pt(dcphen)(ecda)	1.3	0.98	35	3.04	3.40	530	412	0.68	1.10
Pt(dcbpy)(qdt)	0.9	0.89	47	7.00	9.04	600	473	0.77	3.00
Pt(dcphen)(qdt)	0.6	0.88	42	6.50	8.40	550	481	0.72	2.75
Pt(dcphen)(bdt)	0.9	0.66	32	4.72	5.60	543	410	0.70	1.80
Pt(dcbpy)(tdt)	1.0	0.61	6	1.00	1.74	483	301	0.72	0.34
Pt(dcphen)(tdt)	1.1	0.76	20	3.04	3.32	508	404	0.71	1.15

[a] TiO_2 thin films = 16 μm; light source = solar simulator AM 1.5 (100 mW/cm^2); electrolyte = 0.6 M DMPII + 0.05 M I_2 + 0.5 M TBP + 0.1 M LiI in acetonitrile; surface area of electrodes = 0.25 cm^2. [b] Spectroscopically determined surface coverage of the complex. [c] Light-harvesting efficiency at a wavelength of maximum absorbance. [d] Surface area of electrodes: 1.0 cm^2. [e] Electrolyte: 0.6 M DMPII + 0.05 M I_2 + 0.1 M LiI in acetonitrile.

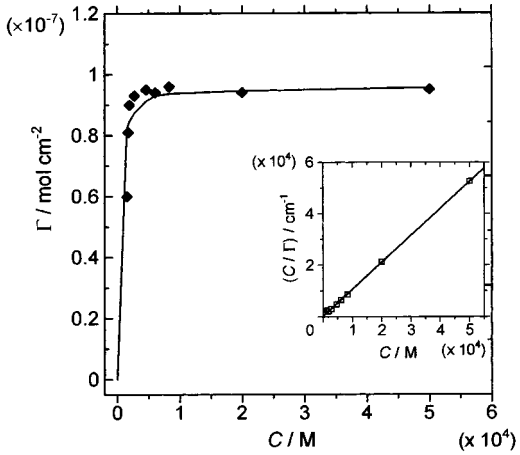

Figure 4. Adsorption isotherm for the sensitizer Pt(dcbpy)(qdt) bound to TiO_2. The inset shows the plot based on the Langmuir adsorption model, where C is the dye concentration in the solution and Γ is the quantity of adsorbed dye.

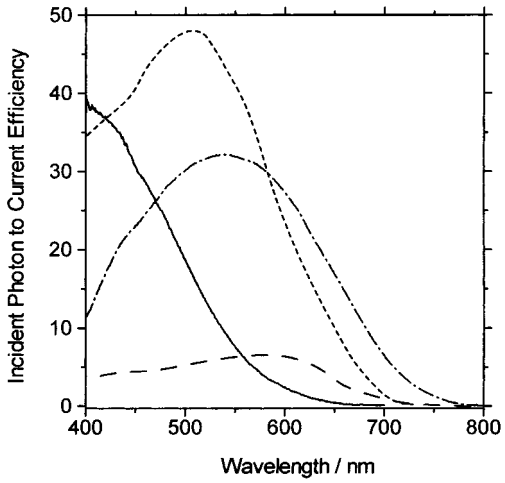

Figure 5. Photocurrent action spectra of nanocrystalline TiO_2 films sensitized by complexes Pt(dcbpy)(ecda) (—), Pt(dcbpy)(qdt) (- - -), Pt(dcphen)(bdt) (— · —), and Pt(dcbpy)(tdt) (— — —). The incident photon-to-current conversion efficiency is plotted as a function of wavelength. A sandwich-type cell configuration was used to measure these spectra.

for the Pt(dcphen)(dithiolate) series of complexes differed by approximately 130 nm in an ethanol/methanol solution (Table 1). Tdt and bdt complexes in ethanol/methanol and adsorbed on TiO_2 films exhibited a low-energy CT absorption band centered at ca. 600 nm (Table 2), which can overlap the solar emission spectrum more efficiently than the CT absorption bands of the ecda and qdt complexes. The broad features of the CT absorption band of Pt(dcbpy)(tdt) covered the entire visible spectrum (Figure 1).

3.6. Langmuir Isotherm for the Adsorption of Pt(dcbpy)(qdt) at the Surface of TiO_2. Adsorption studies of Pt(dcbpy)(qdt) were carried out on TiO_2 films of a known thickness. The dye solution was prepared in ethanol. The amount of dye adsorbed as a function of the equilibrium concentration in the solution is shown in Figure 4. An analysis based on the Langmuir adsorption isotherm model[13g] yielded an estimate of the adsorption equilibrium constant of $K_b = 4 \times 10^{-5}$ M^{-1} for Pt(dcbpy)(qdt). This high adsorption constant value implies a strong interaction between Pt(dcbpy)(qdt) and the TiO_2 surface.[13g,l] The amount of dye adsorbed at saturation was 9.5×10^{-8} mol/cm^2. If we assume that each dye molecule occupies an area of 100 Å,[2,13g,l,39] the inner surface of the film is 550 cm^2 for each 1 cm^2 of geometric surface. Thus, the roughness factor is 550, which is smaller than the experimental value of 1200 obtained from BET experiments for a 12-μm-thick film of TiO_2. One possible explanation for such a difference is that the dye molecules may form linear oligomers through Pt−Pt and ligand−ligand interactions in solution that prevent their penetration into the small pores of the TiO_2 surface.

3.7. Photocurrent Action Spectra of Pt-Dye-Coated TiO_2 Electrodes. Figure 5 shows the photocurrent action spectra for Pt(dcbpy)(ecda), Pt(dcbpy)(qdt), Pt(dcphen)(bdt), and Pt(dcbpy)(tdt) complexes adsorbed on TiO_2 films, where the incident photon-to-current conversion efficiency (IPCE) values are plotted as a function of wavelength. Photocurrent action spectra of each dye-coated TiO_2 electrode collected under short-circuit conditions showed a strong correlation with the absorption spectrum of the metal complex. The maximal IPCE values of all the complexes investigated in this study are given in Table 4. The results described in this section were obtained at high dye-loading levels for which the TiO_2 electrodes were immersed into dye solutions at least 15 h before use. The surface concentrations of the dye samples on TiO_2 films were estimated to be $0.6-1.4 \times 10^{-7}$ mol/cm^2 (Table 4). Square planar Pt(II) complexes are known to exhibit self-quenching[40] and intermolecular-stacking interactions in solution and in the solid state.[25] The dye was coated on TiO_2 electrodes using an ethanolic solution containing 30 mM deoxycholic acid as an additive to avoid surface aggregation of the sensitizer. The presence of a high concentration of additive was found to appreciably increase both the photocurrent and the voltage of the dye-sensitized TiO_2 cells.[13h,l,41] Deoxycholic acid is a steroid derivative that was expected to adsorb onto the TiO_2 surface

(39) Furlong, D. N.; Wells, D.; Sasse, W. H. F. *J. Phys. Chem.* **1986**, *90*, 1107.

(40) (a) Connick, W. B.; Geiger, D.; Eisenberg, R. *Inorg. Chem.* **1999**, *38*, 3264. (b) Connick, W. B.; Gray, H. B. *J. Am. Chem. Soc.* **1997**, *119*, 11620.

(41) Kay, A.; Grätzel, M. *J. Phys. Chem.* **1993**, *97*, 6272.

with its carboxyl and hydroxyl functions and suppress dye aggregation.

The Pt(diimine)(ecda) and Pt(diimine)(qdt) complexes showed similar injection efficiencies at shorter wavelengths, with the Pt(diimine)(qdt) complexes showing an improved response in the red region relative to the ecda complexes. The most efficient sensitizer in this series was the Pt(dcbpy)(qdt), which showed an IPCE value of 47% at 500 nm. However, its light-harvesting capacity at longer wavelengths (>650 nm) was very poor. In contrast, although the red response was improved by changing from Pt(diimine)(qdt) to Pt(diimine)(tdt), the tdt complexes showed very low IPCE values throughout the visible region (Figure 5).

To rationalize these observations, IPCE is expressed in eq 5 in terms of light-harvesting efficiency (LHE), the quantum yield of the charge injection (ϕ_{inj}), and the efficiency of the collection of the injected charge at the back contact (η_c):

$$\mathrm{IPCE} = \mathrm{LHE}(\lambda)\phi_{inj}\eta_c \quad (5)$$

An LHE value of unity is ideal for a solar energy device as it indicates that all the incident radiant power is collected. LHEs at the CT absorption maximum of the studied complexes are given in Table 4. The Pt(diimine)(ecda) and Pt(diimine)(qdt) complexes showed LHEs of ca. 0.9 at the CT absorption maximum. Although the LHE values are close to ideal for these complexes, the IPCE values are only between 35 and 50% for reasons that are discussed in section 3.8. The lower molar extinction coefficients for the Pt(diimine)(tdt) and Pt(dcphen)(bdt) dyes result in lower LHEs (Table 4). The large differences in IPCE values between the Pt(diimine)(qdt) and Pt(diimine)(tdt) dyes cannot be explained only by the small changes in LHE. Therefore, the lower IPCE values of these complexes compared to those of the Pt(diimine)(qdt) complexes cannot be ascribed to low absorbance by these dye-coated electrodes.

The quantum yield of a charge injection is given by

$$\phi_{inj} = k_{inj}/(k_r + k_{nr} + k_{inj}) \quad (6)$$

where k_{inj} is the rate constant for an electron injection from the excited dye to the TiO_2 surface and k_r and k_{nr} are the radiative and nonradiative decays of the excited state in the absence of injection, respectively. The rate of electron injection will occur on an ultrafast time scale if the electronic states are high (i.e., above the conduction band edge) and the electronic coupling between the dye and the semiconductor is large. The excited-state oxidation potentials of these Pt(diimine)(tdt) complexes are sufficiently negative (−1.3 V vs SCE) that they are expected to inject electrons efficiently into the TiO_2 in a fashion analogous to that of the other complexes investigated in this study (Table 3). As stated previously in section 3.4, for the investigated complexes, the excited electron is mainly localized on dcbpy or dcphen in solution because of the lower π^* orbital energy. In all cases of complexes bound via a carboxylic group of dcbpy or dcphen, this suggests an equivalent strength of coupling between the π^* orbital of the dye-excited state and the empty Ti(IV) 3d orbital manifold of the semiconductor. The radiative and nonradiative decays of the excited state compete with electron injection. The rates of the nonradiative decay of the related Pt(diimine)(dithiolate) complexes in a homogeneous solution are reported to be ca. 10^6 s^{-1}.[29] The excited-state lifetimes of all dyes are on the nanosecond time scale, which is ca. 3 orders of magnitude longer than the reported electron injection rate.[14] Nanosecond luminescence decay curves of Pt(dcbpy)(qdt) and Pt(dcbpy)(tdt) attached to a TiO_2 substrate

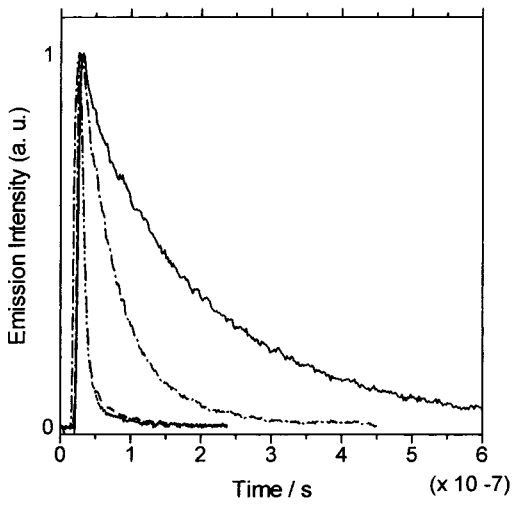

Figure 6. Normalized emission decays for Pt(dcbpy)(qdt) (**5**) and Pt(dcbpy)(tdt) (**8**): (—) **5** in a 4:1 EtOH/MeOH solution, (···) **5** attached to a TiO_2 substrate, (— · —) **8** in a 4:1 EtOH/MeOH solution, and (— — —) **8** attached to a TiO_2 substrate.

are shown in Figure 6. The luminescence decays of both dyes in a 4:1 ethanol/methanol solution are superimposed on the data for comparison. Most of the initial luminescence intensity decays within the laser pulse time (≈7 ns) for both sensitized TiO_2 electrodes. The small contribution of the long-lived component observed in the decay profile of TiO_2-bound sensitizers seems to originate in the sites chemically uncoupled from the TiO_2. Thus, we can conclude that ϕ_{inj} will be high and similar for all the studied sensitized TiO_2 electrodes and that the lower solar energy conversion efficiency observed for the Pt(diimine)(tdt) dyes cannot be adequately explained by either LHE or ϕ_{inj}.

The recombination rates of injected electrons with the oxidized dye are important factors affecting electron collection efficiency (η_c), which falls into the inverted region and will increase as the free-energy change of the electron transfer from the TiO_2 conduction band to the oxidized dye decreases.[42] Alternatively, the recombination rates will increase as the oxidation values change to a more negative potential. On the basis of the measured ground-state oxidation potentials, we expect that the rates of the electron transfer from the conduction band to the oxidized dyes for these complexes will increase in the order of Pt(diimine)(qdt) < Pt(dcphen)(bdt) < Pt(diimine)(tdt). A second channel for charge recombination is the reduction of triiodide to iodide by conduction band electrons. However, this process is very slow under reverse bias, as indicated by the absence of any significant dark current (Figure 7). After electron injection, a competition is set up between charge recombination and iodide oxidation. With the consideration of the relative driving forces of these complexes, the rates of iodide oxidation will increase in the order of Pt(diimine)(qdt) > Pt(dcphen)(bdt) > Pt(diimine)(tdt). As shown in Figure 5, the Pt(dcbpy)(qdt) complex, which has a ground-state oxidation potential that is more positive than that of Pt(dcbpy)(tdt), has an IPCE value of 47% at 500 nm but only 5% for Pt(dcbpy)(tdt). The low IPCE values of the Pt(diimine)(tdt) complexes can be readily explained by the fact that these complexes have the most negative $Pt^{3+/2+}$ ground-state oxidation potentials of all the systems investigated. Thus, they are expected to have the highest relative rate of recombination with electrons from TiO_2 compared to the rate of regeneration by electrons from the electrolyte.

(42) Kuciauskas, D.; Freund, M. S.; Gray, H. B.; Winkler, J. R.; Lewis, N. S. *J. Phys. Chem. B* **2001**, *105*, 392.

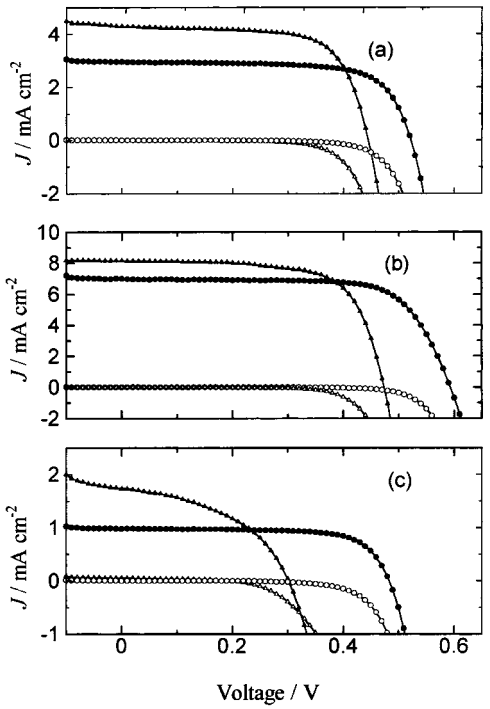

Figure 7. Photocurrent−voltage characteristics of representative TiO_2 electrodes sensitized with dye: Pt(dcbpy)(ecda) (a), Pt(dcbpy)(qdt) (b), and Pt(dcbpy)(tdt) (c). Filled circles and triangles are for illuminations at AM 1.5 solar light with electrolytes with and without TBP, respectively. Open circles and triangles show the dark response with electrolytes with and without TBP, respectively.

3.8. Photocurrent−Voltage Characteristics of Pt-Dye-Coated TiO_2 Electrodes. Figure 7 shows the photocurrent−voltage curves, obtained both in the dark and under AM 1.5 illumination, of the various dye-coated TiO_2 electrode systems investigated in this study. The short-circuit photocurrent density (J_{sc}) and open-circuit voltage (V_{oc}) values for each dye-coated TiO_2 electrode with an electrolyte either containing *tert*-butylpyridine or without *tert*-butylpyridine are reported in Table 4. Table 4 also reports the fill factors (ff) and overall cell efficiencies (η) for the representative samples investigated in this study. The electrolyte containing *tert*-butylpyridine improves the ff and V_{oc} of the device by decreasing the J_{sc}. The increase in the V_{oc} and ff values caused by *tert*-butylpyridine is due to the suppression of the dark current. This can be clearly seen in Figure 7, where the onsets of the dark current are shifted ca. 100 mV by pyridine treatment. Addition of *tert*-butylpyridine, which is basic, to the electrolyte solution moves the conduction band negatively. Thus, the driving force for electron injection is decreased, and the short-circuit photocurrent is also decreased. The most efficient sensitizer in this series was Pt(dcbpy)(qdt), which exhibited a photocurrent of 7.0 mA/cm^2 and an open-circuit potential of 600 mV with an impressive ff of 0.77 under AM 1.5 simulated solar irradiation, corresponding to an overall efficiency of 3.0%. Although the red-shifted absorption spectra of Pt(dcbpy)(tdt) and Pt(dcphen)(tdt) cover the entire visible spectrum of solar light, the observed overall cell efficiency as well as the J_{sc} and V_{oc} values was very low compared to that of Pt(dcbpy)(qdt) (Table 4). The low cell efficiency of these complexes can readily be explained by the high ratios of their rates of recombination and the rates of I^- oxidation, as discussed earlier in section 3.7.

We explored the effect of increased dye surface coverage on the photoelectrochemical properties. Samples were prepared by exposing a TiO_2 electrode to ethanolic Pt(dcbpy)(qdt) solutions of different concentrations containing additives. Photoelectrochemical properties of Pt(dcbpy)(qdt) at different surface coverages are summarized in Table 5. The photocurrents as well as the overall cell efficiency reached a limiting value at a surface coverage of $>9.0 \times 10^{-8}$ mol/cm^2. This may be due to the increased dye aggregation on the TiO_2 film producing an absorptivity that does not inject electrons. Square planar Pt(II) diimine complexes often form dimers and oligomers at high concentrations through Pt−Pt and $\pi-\pi$ stacking.[25] Maximal IPCE values of the TiO_2 electrodes sensitized by ecda and qdt complexes were in the range of 35−50%, though redox potentials of these complexes were obviously in a range that allowed efficient charge injection and dye regeneration. The main reason for the reduced $IPCE_{max}$ values of the ecda and qdt complexes, compared with the most efficient $Ru(dcbpy)_2(NCS)_2$ dye,[13a] was probably surface aggregation that was not completely suppressed, even by the presence of additives. Another possible reason may be self-quenching, which is a general phenomenon of Pt(II) diimine complexes.[40]

Table 5. Dye Concentration Dependence of Photoelectrochemical Properties of Pt(dcbpy)(qdt) Sensitizer[a]

C^b (mol)	$\Gamma \times 10^{-8}$ [c] (mol/cm^2)	LHE[d]	J_{SC} (mA/cm^2)	V_{oc} (mV)	ff	η (%)
1.4×10^{-5}	5.0	0.63	4.0	580	0.74	1.7
1.8×10^{-5}	8.1	0.85	4.4	590	0.74	1.9
2.0×10^{-5}	9.0	0.87	4.7	590	0.72	2.0
2.8×10^{-5}	9.3	0.88	5.3	580	0.70	2.3
4.6×10^{-5}	9.5	0.89	6.0	570	0.73	2.3
5.0×10^{-4}	15.0	0.98	6.0	570	0.70	2.3

[a] TiO_2 thin films = 12 μm; light source = solar simulator AM 1.5 (100 mW/cm^2); electrolyte = 0.6 M DMPII + 0.05 M I_2 + 0.5 M TBP + 0.1 M LiI in acetonitrile; surface area of electrodes = 0.25 cm^2. [b] Dye concentration in an ethanol solution. [c] Spectroscopically determined surface coverage of Pt(dcbpy)(qdt). [d] Light-harvesting efficiency at a wavelength of maximum absorbance.

4. Conclusions

Square planar Pt(II) polypyridyl sensitizers have been synthesized and characterized with dithiolate nonchromophoric ligands. The lowest-energy intense mixed-Pt/dithiolate-to-diimine charge-transfer transitions in these complexes were tuned by ca. 4000 cm^{-1} by changing the donor strength of the dithiolate ligands to extend the spectral response of nanocrystalline TiO_2 photoelectrodes to longer wavelengths. The Langmuir isotherm for the adsorption of Pt(dcbpy)(qdt) at the surface of TiO_2 films showed a low surface coverage that was probably due to dye aggregation in solution. In a solar cell arrangement, these sensitizers efficiently convert light into electricity over the entire visible region. A short-circuit photocurrent of 7.0 mA/cm^2 and an open-circuit potential of 600 mV with an impressive fill factor of 0.77 were obtained for Pt(dcbpy)(qdt) under AM 1.5 simulated solar irradiation, corresponding to an overall efficiency of 3%. A sluggish halide oxidation rate, a fast recombination of the injected electron with the oxidized dye, or both were likely responsible for the low cell efficiency observed for Pt(dcbpy)(tdt) and Pt(dcphen)(tdt).

Acknowledgment. We acknowledge Prof. Takeshi Ohno of the University of Osaka for useful discussions. Financial support of this work from the Science and Technology Agency, Center of Excellence Development Project (COE), Japan, is gratefully acknowledged.

IC010391Y